Methods for Initialization of Activation Based Inverse Electrocardiography Using Graphs Derived from Heart Surface Geometry

B Erem[1], PM van Dam[2], A Keely[3], JG Stinstra[4],
TF Oostendorp[2], DH Brooks[1]

[1]Northeastern University, Boston, MA, USA
[2]Radboud University Medical Centre, Donders Centre for Neuroscience, Nijmegen, NL
[3]Nuance Communications, Inc., Burlington, MA, USA
[4]University of Utah, Salt Lake City, UT, USA

Abstract

The activation-based inverse problem of electrocardiography is non-linear in the desired activation times. Current solutions rely on iterative algorithms. There is considerable interest in improved initialization approaches due to the importance of the initialization used. Recent efforts include the critical point algorithm of Huiskamp and Greensite and the fastest route algorithm of van Dam, Oostendorp, and van Oosterom. In this work we analyze the relationship between these two methods. We also suggest an alternative to the shortest path approach to represent the set of likely activation patterns that may have computational advantages. We also explore modifications to these two methods exploiting their relationship and using the new activation patterns. We use epicardially stimulated data and geometries, recorded at the Cardiovascular Research and Training Institute in Utah, and geometries and forward matrix supplied with the ECGSim software, to compare results.

1. Introduction

The activation-based inverse problem of electrocardiography is to find the activation (depolarization) times of nodes on the heart from body surface potential (BSP) observations and is non-linear in the desired activation times. Current solution methods rely on iterative algorithms and the results are typically highly dependent on the initialization used. Thus there has been considerable interest in improved initialization approaches such as the shortest path - fastest route methods of van Dam, Oostendorp, and van Oosterom and the critical point method of Huiskamp and Greensite[1–7].

In this work, we begin with an introduction to the fastest route and critical point algorithms, analyze the relationship between them, and explain how they can combined advantageously. We suggest an alternative to the shortest path (fastest route) approach to finding candidate activation patterns on the heart, based on the geometry, and use these activation patterns to introduce modifications to the fastest route and critical point algorithms to create two new algorithms. We compare results for a variety of activation patterns for epicardially stimulated data recorded at the Cardiovascular Research and Training Institute in Utah, and converted to the geometries supplied along with the ECGSim software.

2. Methods

Our algorithms are modifications to two existing algorithms: the fastest route algorithm and the critical point algorithm. First we will introduce the existing methods, discuss their relationship, and suggest a modification to each one that takes advantage of this relationship.

2.1. Fastest route algorithm (FRA)

The fastest route algorithm uses the heart geometry to derive likely activation patterns and then compares the body surface potentials predicted by each such pattern to measured data using a correlation approach [1, 2]. In this single-activation case, in Table 1, the heart geometry's nodes V and edges E are treated as a graph $G = (V, E)$, and candidate activation patterns are derived as shortest path propagations along the graph's edges. In the multiple-activation case, not explained in detail here, multiple such patterns are combined to create more complex activation sequences using a "first-come, first-served" approach [3, 4]. In both cases, the pattern that serves as the initialization for the iterative solution is that whose

Table 1. Single-Activation Fastest Route Algorithm

	Given: Heart graph G, propagation speed ν, initial activation time t_0, BSPs Y, forward matrix A
1.	Find the shortest paths through G from every node
2.	Calculate candidate activation timings P from shortest paths assuming unit propagation speed
3.	Adjust duration and start times by multiplying by ν and adding t_0 to the timings in P
4.	Form a candidate activation matrix H_i for every P_i in P s.t. its rows are smoothed step functions phase-shifted by the timings in P_i
5.	Choose the initialization τ as the P_i that results in the highest correlation between Y and AH_i

Table 2. Critical Point Algorithm

	Given: BSPs Y, forward matrix A Let: $f_{\text{eval}}(U_t, i) = \left(1 - \frac{A'_{:,i} U_t U_t{}' A_{:,i}}{\|A_{:,i}\|_2^2}\right)^{-1}$
	First do (1-3) for every node i and every time t:
1.	Create Y_t^- and Y_t^+ as the past and future BSPs
2.	Find their noise subspaces U_t^- and U_t^+ from SVD
3.	Calculate zero-crossing matrix Z as $Z_{i,t} = f_{\text{eval}}(U_t^-, i) - f_{\text{eval}}(U_t^+, i)$
4.	Choose the initialization τ such that every τ_i equals the t at which $Z_{i,t}$ crosses zero

forward-predicted BSPs have the highest correlation with the observed BSPs.

2.2. Critical point algorithm (CPA)

The critical point algorithm, in the implementation commonly in use in Table 2, projects single-node activations onto the noise subspace of the data. Small projections indicate nodes which "initiate" local activation spread, along with the associated activation timing [6,7]. In effect the assumption is that the final activation sequence is the superposition of independent single-node activations. This can be seen in the f_{eval} function, which is based on projecting single columns of the forward matrix A into the noise subspace U_t. In this implementation, the initialization for the iterative solution comes from determining when, in time, the presence of a single node's forward contribution transitions from the future (the subspace for the later data, U_t^-) to the past (the subspace for the earlier data, U_t^+), which is equivalent to finding the zero-crossings in the Z matrix for each node.

2.3. Relationship between FRA and CPA

FRA and CPA both rely on two common parts: activation pattern generation and evaluation. As explained above, FRA generates patterns using a shortest path search, enforcing spatial regularity that CPA, which generates single activations of each node, may be missing. Furthermore, FRA evaluates each pattern using a correlation measure, whereas CPA evaluates by projecting into relevant subspaces. By borrowing from another method's generation or evaluation parts, or otherwise modifying them, either of these methods can potentially be enhanced.

2.4. Modifications to existing methods

To demonstrate their relationship, we modified each algorithm such that they share a new generation step in common, and also adjusted the evaluation step of CPA to take advantage of such a change.

Activation pattern matrix: We use a geometrically-derived activation pattern matrix, W, as an alternative to the shortest path search, to represent the set of likely activation patterns to be tested. Each element of the matrix is a weight between nodes m and n on the heart and is assigned as

$$W_{m,n} = \exp\left(-d_{m,n}^2/(2\sigma^2)\right)$$

where $d_{m,n}$ is the Euclidean distance between the nodes, and σ is a parameter which controls the width of the inverse exponential function. We then normalize each column n of W by its maximum value,

$$W_{:,n} \leftarrow W_{:,n}/\max(W_{:,n})$$

so that those elements corresponding to nodes close to n are 1 and exponentially decay to 0 for those further away.

In this form, the columns of W are spatial windows used to modify CPA. However, with a small modification to these windows, we can create candidate activation patterns to modify FRA. When subtracted from a vector of ones, each column of W is a "normalized" activation pattern that can be scaled to the desired duration and added to a constant so that the pattern starts at the desired time.

Modified FRA: In the case of FRA, the primary purpose of our modification is to be able to obtain similar results to the single-activation FRA with a simple alternative to running a shortest path algorithm on the graph derived from the heart geometry. This method substitutes the candidate initializations in FRA with those derived from the columns of the W matrix above. Each column of W is then taken as a candidate "shortest path" type pattern, and the correlation to the resulting predicted body surface potentials is used to choose the best pattern. Each column is first subtracted from a vector of ones, scaled by the duration of QRS, T_{QRS}, and then shifted in time by adding a constant, t_0, corresponding to the start of QRS, which we assume to be known in this work, to create a resulting pattern P_i:

$$P_i = T_{\text{QRS}}(1 - W_{:,i}) + t_0$$

For each such candidate P_i, we populate the rows of an activation matrix H_i with smoothed step functions phase-shifted (in the columns, which index time) by the elements of P_i [8]. We choose as τ, our initialization, as whichever candidate forward-predicted BSPs have the highest correlation with the observed BSPs. The only way in which this differs from the standard single-activation version of FRA in Table 1 is the way in which each activation pattern P_i is generated.

Modified CPA: For this method the intention of our modification is to achieve a potential qualitative improvement in the spatial characteristics of the initial estimate, subject to choice of σ parameter. This method substitutes the single-node activations in CPA with the spatial windows in the columns of the W matrix. So rather than projecting a single column of A into the noise subspace, this method projects a linear combination of the columns of A weighted by the window, thus imposing some spatial regularity on the method. To be more specific, the evaluation function becomes

$$f_{\text{eval}}(U_t, i) = \left(1 - \frac{(AW_{:,i})' U_t U_t' (AW_{:,i})}{\|AW_{:,i}\|_2^2}\right)^{-1}$$

and the rest remains the same as the critical point algorithm in Table 2. We note that when $W = I$, the identity matrix, this algorithm reduces to the critical point method.

2.5. Experiments

To experiment with our methods, we used epicardially stimulated data recorded on the epicardium of a canine heart at the Cardiovascular Research and Training Institute (CVRTI) in Utah. We calculated the activation times from the recorded data, and projected these values from the geometry of the Utah epicardium to just the epicardium of the Nijmegen heart, the default geometry provided by ECGSim (which also provides the corresponding forward matrix) [9]. We completed the activation timings on the Nijmegen heart by propagating the values to the endocardium using SCIRun [10]. We simulated the corresponding BSPs by forward-computing them from our activation times and adding noise with a signal-to-noise ratio (SNR) of 30 dB. Thus our experiments consisted of running the various initialization methods on the Nijmegen geometries with this set of data, converted from data recorded on different geometries in Utah using a set of data conversion methods.

3. Results

For these experiments, we chose values of σ such that it was parameterized by β as $\sigma = \beta d_{\text{min}} + (1-\beta) d_{\text{max}}$, where d_{min} and d_{max} are the minimum and maximum distances between nodes in the geometry, respectively. Results were visualized with *map3d* [11]. The activation pattern matrix is a substitute for the shortest path search in FRA. As Figure 1 shows, similar results can be obtained by several activation patterns generated using our method (β = 0.5, 0.6, 0.7, 0.8). Figure 2 shows the results of modified CPA for a range of β values. By changing the β parameter in the modified version of CPA, one can obtain initializations of varying spatial regularity. We can see that the contour lines show a gradual change in the shape of the resulting activation patterns as β is increased, until the result for $\beta = 0.95$ is nearly the same as CPA itself. Comparing these to the true timings in Figure 1, we see that the modified version of CPA has certain shapes in its contours that are missing from CPA.

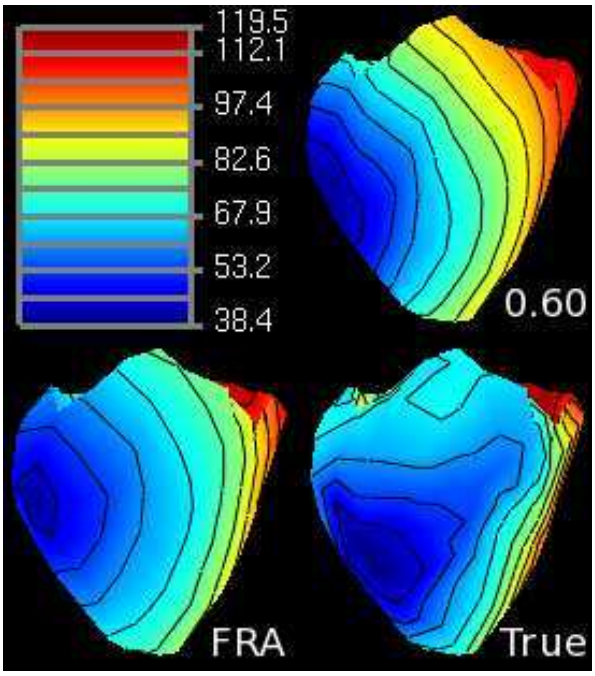

Figure 1. Results of FRA, its modified version ($\beta = 0.6$ chosen from generated $\beta = 0.5, 0.6, 0.7, 0.8$) , and the true activation times.

4. Discussion and conclusions

In this work, we have explained the relationship between two recent methods for initializing iterative solutions to the activation-based inverse problem of electrocardiography, suggested a new method for generating activation patterns, W, and modified the two related algorithms to create new ones. A simple modification to our method would allow for W to account for varying propagation speeds, as sometimes done in FRA. However, we still need to consider how our generation method can be used to combine multiple activations. As for CPA, any other method to create W can be

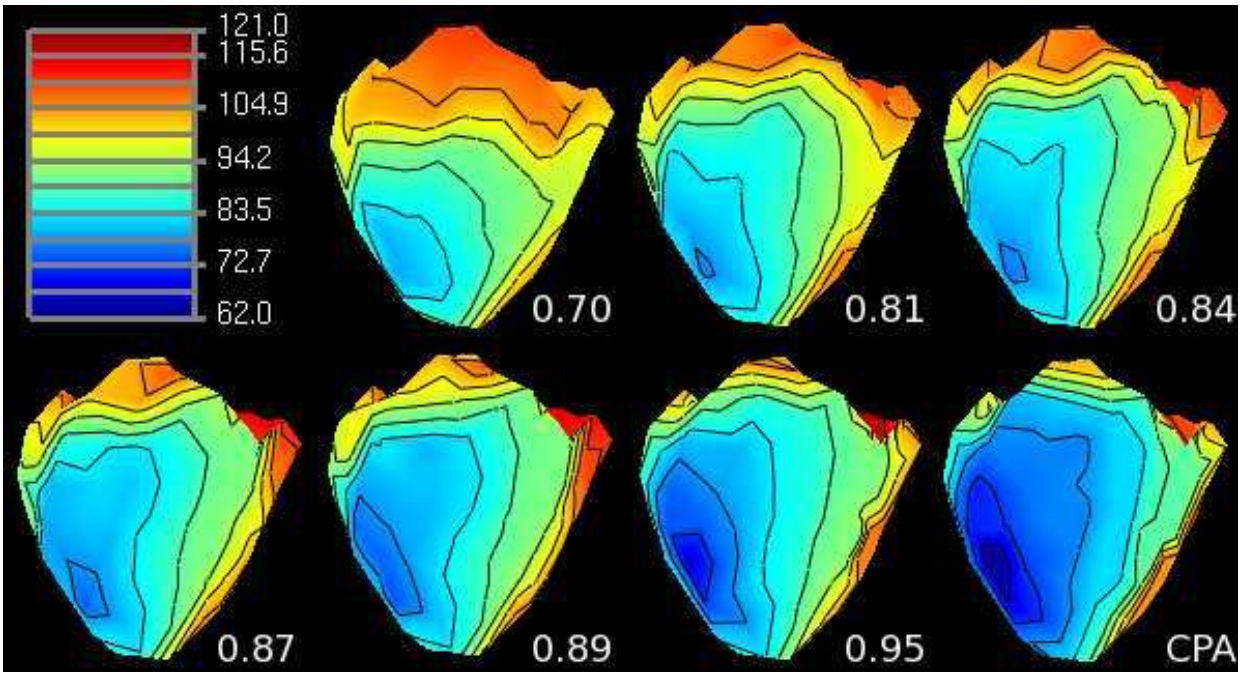

Figure 2. Results of CPA and modified values of $\beta = 0.7$, 0.81, 0.84, 0.87, 0.89, and 0.95.

used to modify it in a similar way, with possibly improved results. Finally, we have used two different open software packages, including open conversion routines that we intend to make available soon, along with freely available datasets and geometries in this work. Now we can compare results in a common software framework with common data and we hope that our effort will contribute to a goal of increasing reproducibility and interoperability of research efforts in inverse electrocardiography.

Acknowledgements

This work was made possible in part by the NIH/NCRR Center for Integrative Biomedical Computing, P41-RR12553-10.

References

[1] van Oosterom A, van Dam P. The intra-myocardial distance function used in inverse computations of the timing of depolarization and repolarization. Computers in Cardiology 2005 2005;567–570.

[2] van Dam P, Oostendorp T, van Oosterom A. Simulating ECG Changes during Acute Myocardial Ischemia. Computers in Cardiology 2007 2007;325–328.

[3] van Dam P, Oostendorp T, van Oosterom A. Application of the fastest route algorithm in the interactive simulation of the effect of local ischemia on the ECG. Medical and Biological Engineering and Computing 2009;47(1):11–20.

[4] van Dam P, Oostendorp T, Linnenbank A, van Oosterom A. Non-invasive imaging of cardiac activation and recovery. Annals of Biomedical Engineering 2009;1–18.

[5] Huiskamp G, Greensite F. A new method for myocardial activation imaging. IEEE Transactions on Biomedical Engineering 1997;44(6):433–446.

[6] Pullan A, Cheng L, Nash M, Bradley C, Paterson D. Non-invasive electrical imaging of the heart: theory and model development. Annals of Biomedical Engineering 2001; 29(10):817–836.

[7] Pullan A, Cheng L, Buist M. Mathematically Modelling the Electrical Activity of the Heart: From Cell to Body surface and back again. World Scientific Pub Co Inc, 2005.

[8] Huiskamp G, Van Oosterom A. The depolarization sequence of the human heart surface computed from measured body surface potentials. IEEE Transactions on Biomedical Engineering 1988;35(12):1047–1058.

[9] Van Oosterom A, Oostendorp T. ECGSIM: an interactive tool for studying the genesis of QRST waveforms, 2004.

[10] SCIRun: A Scientific Computing Problem Solving Environment, Scientific Computing and Imaging Institute (SCI).

[11] Map3d: Interactive scientific visualization tool for bioengineering data. Scientific Computing and Imaging Institute (SCI).

Address for correspondence:

Burak Erem
360 Huntington Avenue
Northeastern University, 409 Dana Building
Boston, MA 02115, USA
berem@ece.neu.edu